Journal of Applied Sciences

ISSN 1812-5654

science alert

ANSInet
an open access publisher
http://ansinet.com

Journal of Applied Sciences 10 (15): 1580-1587, 2010
ISSN 1812-5654

An Analytical Approach of the Behavior of Fiber Reinforced High Shrinkage Materials

[1]N. Shatarat, [2]Bassel J. Hanayneh and [1]H. Katkhuda
[1]Department of Civil Engineering, The Hashemite University, Zarqa, Jordan
[2]Department of Civil Engineering, University of Jordan, Amman, Jordan

Abstract: This study presents an analytical approach to predict the behavior of fiber-reinforced materials with high shrinkage properties. A simple model formed of a rigid fiber embedded in a cylindrical elastic matrix presenting high shrinkage properties was analyzed. Isotropy and homogeneity of the two constituents, the fiber and matrix, as well as the shrinkage of the matrix were assumed for simplification. The analytical analyses included the variations of the state of link at the fiber-matrix interface due to its effect on the global behavior of fiber-reinforced material. The study showed the effect of the bond strength on the bond length, the effect of the bond length on free shrinkage, the effect of the age of the composite material on the bond length and the effect of the fiber volumetric fraction on the equivalent mean length.

Key words: Fiber-reinforced concrete, bond stress, bond length, cracking, shrinkage, metal fibers

INTRODUCTION

Fibers are most often added to cement composites to improve their fracture behavior. This concept of reinforcement was used in building materials in the old days. There is an evidence that asbestos fiber was used to reinforce clay posts about 5,000 years ago.

The behavior of composite materials formed of a given binder and a matrix presenting high shrinkage properties is much related to the state of interlocking, mechanical or chemical between the fiber and matrix. If the bond is perfect the shrinkage will be inhibited. In this case the behavior of the material vis-à-vis the tensile strength and consequently the shrinkage induced cracking is not known, whereas if plain fibers are used the shrinkage would not be inhibited but the tensile strength of the resulting composite material would be improved (Toledo Filho *et al*., 2005).

The modeling of fibers and the bond properties for fibers in fiber reinforced concrete has received much attention in the literature in the past several decades. Nammur and Naaman (1989) derived an analytical model of the bond shear stresses at the fiber-matrix interface in a pure tensile fiber reinforced concrete specimen. The derived model predicted the shear stress distribution along the fiber-matrix, the slip distribution and the normal tensile stresses in the fiber and the matrix. Perfect alignment of the fibers as well as square packing was assumed. The model was finally used to predict numerically the bond shear stress in a given tension composite using a specific bond-slip curve.

In a previous work performed by Hanayneh (1994), a parametric analysis of the fiber-matrix interface in materials with high shrinkage properties was studied numerically. The study showed the influence of some parameters on the behavior of an elementary model. However, the applications of this type of analysis were of limited use. Li and Li (2001) modeled the behavior of fiber reinforced concrete based on the Continuum Damage Mechanics. In the material, a cement-sand-coarse-aggregate-water mix was used as the matrix and short steel fibers were used as the reinforcement. The quasi-brittleness of the matrix and the fiber-matrix interfacial properties were taken into consideration. Results show that the model-predicted stress-strain curves agreed well with those obtained experimentally.

Lately, many researchers applied experimental programs to study the use of fiber- reinforced to reduce plastic shrinkage in concrete (Boghossian and Wegner, 2008; Sivakumar and Santhanam, 2007; Passuello *et al*., 2009).

On the other hand, Boulekbache *et al*. (2010) investigated the fiber distribution and orientation by using a translucent fluid model with a yield stress. The observation confirmed the ability of the developed method to provide data on the orientation and distribution of steel fibers within concrete. It was showed that orientation and distribution are dependent on the yield stress of the fluid material. The flexural strength depends on the fiber distribution and orientation and is significantly improved when the fibers are oriented in the direction of the tensile stresses fresh (concrete with good

Corresponding Author: Nasim Shatarat, Department of Civil Engineering, The Hashemite University, P.O. Box 150459, Zarqa 13115, Zarqa, Jordan Tel: +962(5)390333 Fax: +962(5)3826348

workability). On the contrary, for concrete with poor workability, an inadequate orientation of fibers occurred, leading to a poor contribution of the fibers to the flexural behavior of the tested specimens, despite the relatively higher compression strength of the tested concrete material.

Jay Kim *et al.* (2008) constructed reinforcing fibers with three different geometries, i.e., embossed, straight and crimped, from waste polyethylene terephthalate (PET) bottles and used them to control plastic shrinkage cracking in cement-based composites. Pullout tests evaluated how the fiber geometry and fraction by volume (0.1-1.00%) affected the rate of moisture loss and controlled the plastic shrinkage cracking characteristics

Barluenga (2010) demonstrated that inclusion of small amounts of short fibers has an effective solution to control cracking due to drying shrinkage of concretes at early ages. The key point of fiber effectiveness is their capacity to sew the crack sides, preventing crack opening, because cracking of concrete matrix induces fiber actuation. The results showed that as concrete mechanical capacity develops with age, while fibers have full properties before being included in concrete matrix, the interphase between matrix and fibers evolves during setting and hardening and affects cracking control effectiveness, due to stresses induced by fibers into the matrix during concrete hydration.

Other researchers such as Leung *et al.* (2006) used shotcrete and fiber reinforced shotcrete to produce layers or linings with large surface area versus volume ratios to restrain shrinkage cracking. A new testing configuration, consisting of a shotcrete specimen bonded to a steel I-section and angles was proposed. From the results, the proposed set-up is shown to be a practical and viable approach for investigating the shrinkage cracking behavior of shotcrete and fiber reinforced shotcrete.

Most of the existing models presented in the literature are relatively complicated. On the other hand, the extensive use of fiber reinforced composite materials made it necessary to come up with a material model that can be easily incorporated into existing design procedures for professional engineers. This paper proposes a simple analytical approach that was developed by the authors in Jordan on a research project that started on July 2008 and ends on March 2010, which would allow the analysis and the study of the behavior of fiber-reinforced materials with high shrinkage properties by varying the parameters related to the fibers and the matrix. A model formed of a rigid fiber embedded in a cylindrical elastic matrix presenting high shrinkage properties is analyzed. Deformations of the matrix are assumed not to lead to deformations in the fibers. Thus, the analytical model presented in this study is most appropriately applicable to cases of stiff fibers.

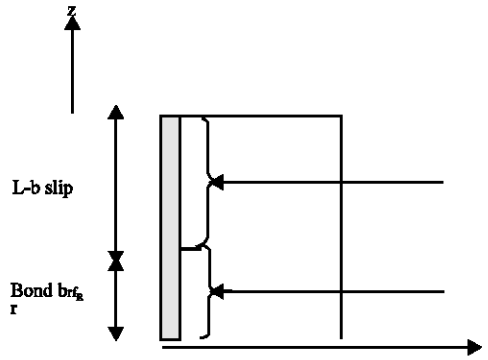

Fig. 1: Representation of the cylindrical model used in the study

DESCRIPTION OF THE MODEL

The model consists of two coaxial cylinders of radii r_f and R, respectively, as shown in Fig. 1. The inner cylinder represents the rigid fibers with a radius of r_f and the outer cylinder represents the matrix at a radius equal to R. The length of the model is equal to L and the length of the bond between the fibers and the matrix is assumed to be equal to b. Since the cylinder is symmetrical, it will be sufficient for further calculations to consider one quarter of the cylinder as shown in Fig. 1.

Assumptions: To simplify the study of the model, the following assumptions are adopted:

- Isotropy and homogeneity of the two constituents: the fiber and matrix
- Rigidity of the fiber, i.e., deformations of the matrix does not necessarily lead to deformations in the fiber. This assumption limits the applicability of the approach to cases of stiff fibers
- Isotropy of the shrinkage of the matrix

PROBLEM FORMULATION

Equilibrium equations: The deformations of the cylinder are symmetrical around the z-axis. The stresses are independent of θ and consequently all their derivatives with respect to θ are equal to zero. The shear stresses $\sigma_{r\theta}$ and $\sigma_{\theta z}$ cancel one another by virtue of symmetry. The equilibrium equations in cylindrical coordinate system, therefore, are limited to:

$$\frac{\partial \sigma_{rr}}{\partial_r} + \frac{\partial \sigma_{rz}}{\partial_z} + \frac{\sigma_{rr} - \sigma_{\theta\theta}}{r} = 0 \quad (1)$$

$$\frac{\partial \sigma_{rz}}{\partial r} + \frac{\partial \sigma_{zz}}{\partial z} + \frac{\sigma_{rz}}{r} = 0 \quad (2)$$

Constitutive laws-shrinkage: If a material is anisotropic, its shrinkage, if any, will necessarily be anisotropic too. Depending upon the dimensions of the sample, shrinkage can equally be heterogeneous and hence a shrinkage gradient develops: the outer parts of the sample shrink more than the inner parts at any given moment of time.

As far as the above model is concerned, it will be assumed that shrinkage is isotropic. On the other hand, since its dimensions are assumed to be small, shrinkage will be assumed to be homogeneous. Consequently, shrinkage does not depend on coordinates r, z, θ but only on time. Proceeding in a manner similar to classical thermo elasticity, the term for thermal expansion will be replaced by a term called shrinkage.

In the absence of stresses, anisotropic shrinkage $\bar{\varepsilon}$ results in a contraction:

$$\varepsilon_{ij} = \bar{\varepsilon} \times \delta_{ij}$$

with $\bar{\varepsilon}$ considered here to be dependent only on time. On the other hand at time t_0, for reference shrinkage $\bar{\varepsilon}_0$, the material is assumed to behave as an elastic isotropic material with Poisson's ratio v and modulus of elasticity E. Therefore, in a simplified manner, the shrinkage of the matrix becomes:

$$\varepsilon_{ij} = \frac{1+\nu}{E}\sigma_{ij} - \frac{\nu}{E}\sigma_{kk}\,\delta_{ij} + \bar{\varepsilon}\delta_{ij}$$

and inversely the stresses are:

$$\sigma_{ij} = \lambda \varepsilon_{kk}\,\delta_{ij} + 2\mu\varepsilon_{ij} - 3k\bar{\varepsilon}\delta_{ij}$$

where, $3k = 3\lambda + 2\mu$ with $\mu = E/2(1+v)$, $\lambda = v/(1-2v)(1+v)$, $3k = E/(1-2v)$ and in a system of cylindrical coordinates, the non-zero stresses at time t are:

$$\sigma_{rr} = \frac{E}{(1+v)(1-2v)}\left[(1-v)\,\varepsilon_{rr} + v(\varepsilon_{\theta\theta} + \varepsilon_{zz}) - (1+v)\bar{\varepsilon}\right] \quad (3)$$

$$\sigma_{\theta\theta} = \frac{E}{(1+v)(1-2v)}\left[(1-v)\,\varepsilon_{\theta\theta} + v(\varepsilon_{rr} + \varepsilon_{zz}) - (1+v)\bar{\varepsilon}\right] \quad (4)$$

$$\sigma_{zz} = \frac{E}{(1+v)(1-2v)}\left[(1-v)\,\varepsilon_{rr} + v(\varepsilon_{\theta\theta} + \varepsilon_{zz}) - (1+v)\bar{\varepsilon}\right] \quad (5)$$

$$s_{rz} = \frac{E}{2(1+v)}\varepsilon_{rz} \quad (6)$$

It is observed that the expressions for normal stresses cancel one another for $\varepsilon_{rr} = \varepsilon_{zz} = \varepsilon_{\theta\theta} = \bar{\varepsilon}$. This is the case of free shrinkage. On the other hand, for a symmetrical deformation, the deformation-displacement relationships are:

$$\varepsilon_{rr} = \frac{\partial U_r}{\partial r} \quad (7)$$

$$\varepsilon_{\theta\theta} = \frac{U_r}{r} \quad (8)$$

$$\varepsilon_{zz} = \frac{\partial U_z}{\partial z} \quad (9)$$

$$\varepsilon_{rz} = \frac{1}{2}\left(\frac{\partial U_r}{\partial z} + \frac{\partial U_z}{\partial r}\right) \quad (10)$$

The equilibrium Eq. 1 and 2, expressed in terms of displacements, are:

$$\frac{\partial^2 U_r}{\partial r^2} + \frac{1}{r}\frac{\partial U_r}{\partial r} - \frac{U_r}{r^2} + \frac{(1-2\nu)}{2(1-\nu)}\frac{\partial^2 U_z}{\partial z^2} + \frac{1}{2(1-\nu)}\frac{\partial^2 U_z}{\partial r \partial z} = 0 \quad (11)$$

$$\frac{\partial^2 U_z}{\partial r^2} + \frac{2(1-\nu)}{(1-2\nu)}\frac{\partial^2 U_z}{\partial z^2} + \frac{1}{r}\frac{\partial U_z}{\partial r} + \frac{1}{(1-2\nu)}\frac{\partial U_r^2}{\partial r \partial z} + \frac{1}{(1-2\nu)}\frac{1}{r}\frac{\partial U_r}{\partial z} = 0 \quad (12)$$

Variation of the state of link at the fiber matrix interface

Bond length and slip length: The study of the variations of the state of link at the fiber-matrix interface has its importance due to its effect on the global behavior of fiber-reinforced material. A case of perfect bond is assumed to take place if the mean bond strength τ_b, determined experimentally, is higher than the shear stress σ_{rz}; otherwise, slip along the fiber prevails. The modulus of elasticity E and Poisson's ratio v will be assumed to be known and having constant values.

Determination of the shear stress σ_{rz}: The shear stress σ_{rz} is developed in the matrix due to its inherent shrinkage and to due to the presence of rigid fiber itself. The shear stress σ_{rz} can be determined using the displacement Eq. 3-10.

Determination of the displacements U_r, U_z and the shear stress σ_{rz}: An approximate solution of the equilibrium Eq. 11-12 which satisfies the boundary conditions in displacements which impose that in the case of perfect bond at the interface, $U_r(r_f, z) = 0$ and $U_z(r_f, z) = 0$ was found in the following forms:

$$U_r = k_1\left(r - \frac{r_f^2}{r}\right) \quad (13)$$

$$U_z = k_2\left[k_3 \ln\frac{1}{r} + k_4\left(1 - \frac{r_f}{r}\right)\right]z \quad (14)$$

where, the coefficients k_1 to k_4 can be determined using the results obtained from the numerical method. These values are: $k_1 = 1.1\varepsilon$, $k_2 = \varepsilon$, $k_3 = 0.25$ and $k_4 = 0.21$. The shear stress σ_{rz} can be found using Eq. 6, which gives:

$$\sigma_{rz} = -\frac{E\varepsilon}{2(1+\nu)}\left(-\frac{0.25}{r} + 0.21\frac{r_f}{r^2}\right)z \quad (15)$$

which yields at the interface ($r = r_f$)

$$\sigma_{rz} = \frac{0.02E\varepsilon}{(1+\nu)r_f}z \quad (16)$$

Determination of the bond length b: Following, perfect bond takes place in the case where:

$$\frac{0.02E\varepsilon}{(1+\nu)r_f}z < \tau_b$$

which yields:

$$z < \frac{(1+\nu)\tau_b r_f}{0.02E\varepsilon} \quad (17)$$

if the length of the cylindrical model L is introduced, Eq. 17 becomes:

$$\frac{b}{L} < \frac{1+\nu}{0.02}\frac{\tau_b}{E\varepsilon}\frac{r_f}{L} \quad (18)$$

Hence, the following three cases of the state of link can be identified:

- $\frac{b}{L} = 0$ Case of total sliding along the fiber length
- $\frac{b}{L} = 1$ Case of perfect bond along the fiber length
- $0 < \frac{b}{L} < 1$ Case of perfect bond along b and sliding along (L – b)

Effect of the bond strength τ_b on the bond length b: The values considered in this paragraph are taken from a previous work (Hanayneh, 1994): E = 600 MPa, v = 0.175, r_f = 0.4 mm, L = 42 mm and $\varepsilon = 5\text{x}10^{-4}$. Thus, Eq. 18 becomes:

$$\frac{b}{L} < 1.87\tau_b \quad (19)$$

Figure 2 as well as Eq. 19 show that the bond length increases as the bond strength at the interface increases.

Effect of shrinkage on the bond length: Let the value of the bond strength τ_b= 0.2 MPa and keep the values of the other parameters E, v, r_f, L and ε the same as in the previous section, then Eq. 18 becomes:

$$\frac{b}{L} < \frac{1.87\times10^{-4}}{\varepsilon} \quad (20)$$

This equation as well as Fig. 3 shows that the bond length is inversely proportional to shrinkage, given that the bond strength at the interface is constant.

Effect of age on the bond length: Although the modulus of elasticity and Poisson's ratio undergo slight variation with time, they are assumed to be constant in this study. The following relationships relating the effect of age on the bond strength τ_b and free shrinkage ε are used:

$$\tau_b = 0.0155\sqrt{t} + 7.74\times10^{-3}t^{3/4} + 0.115 \quad (21)$$

$$\varepsilon = 1.333\sqrt{t} - 0.385t^{3/4} \quad (22)$$

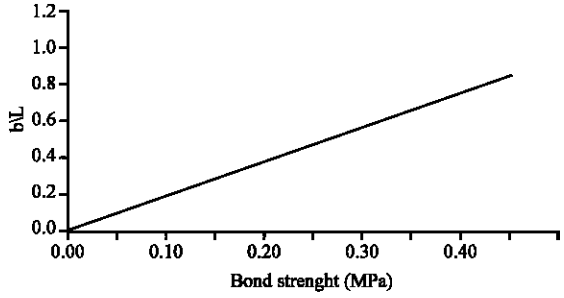

Fig. 2: Effect of the bond strength on the bond length

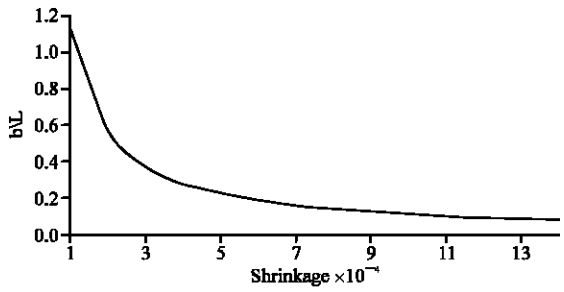

Fig. 3: Effect of shrinkage on the bond length

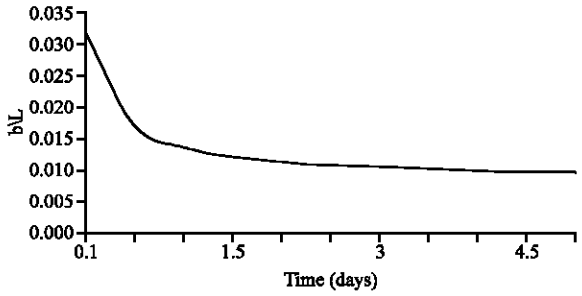

Fig. 4: Effect of age on the bond length

where, t is the time in days.

Reporting the previous relationships into Eq. 19 gives:

$$\frac{b}{L} < \frac{0.993\times10^{-3}\left(0.01555\sqrt{t} + 7.74\times10^{-3}t^{3/4} + 0.115\right)}{1.333\sqrt{t} - 0.385t^{3/4}} \quad (23)$$

Equation 23 is represented in Fig. 4. It shows that the bond length decreases as age increases, however, this behavior does not mean that fiber reinforced materials become weaker. In fact, this depends upon the tensile strength of the matrix and the bond strength at the interface.

Estimation of the equivalent mean shrinkage: The idea of introducing the concept of equivalent mean shrinkage to give an adequate approximation of the shrinkage of fiber-reinforced material can be made through studying the behavior of an elementary cell. In fact, the global material can be considered as an assembly of elementary cells in a given direction. Figure 5 shows a representation of such an assembly. In this study, the shrinkage is assumed longitudinal and the reinforcing fibers aligned.

In the model which consists of a rigid fiber embedded in a matrix, the longitudinal shrinkage is not uniform along the section of the cylinder. In fact, it has been shown that the shrinkage of the matrix increases as the distance from the fiber increases. In addition, the shrinkage of the rigid fiber is considered negligible.

The equivalent mean shrinkage will be calculated for the following two cases:

- Perfect bond, $(\varepsilon_{eq})_b$
- Partial slip, $(\varepsilon_{eq})_s$

Case of perfect bond along the whole length: This case is characterized by the following relations:

$$b = L = \frac{1+\nu}{0.02}\frac{\tau_b}{E\varepsilon}r_f$$

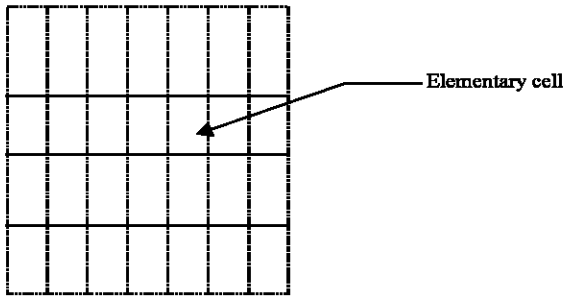

Fig. 5: Assembly of the elementary cells containing the fibers

and

$$(U_z)_b = -\varepsilon\left[0.25\ln\frac{r_f}{r} + 0.21\left(1-\frac{r_f}{r}\right)z\right]$$

Therefore, the equivalent mean shrinkage $(\varepsilon_{eq})_b$ can be written as:

$$(\varepsilon_{eq})_b = \frac{1}{\pi\left(R^2 - r_f^2\right)}\int_{r_f}^{R}\frac{(U_z)_b}{1}2\pi r dr$$

and replacing $(U_z)_b$ by its expression and after integration, the equation becomes:

$$(\varepsilon_{eq})_b = -\frac{2\varepsilon}{R^2 - r_f^2}\left[0.125\,R^2\left(\ln\frac{r_f}{R} + 1.25\right) - 0.21\,r_f\,R + 0.054\,r_f^2\right] \quad (24)$$

Introducing the volumetric fraction $V_f = (r^2_f/R)$ Eq. 24 becomes:

$$(\varepsilon_{eq})_b = -\frac{2\varepsilon}{1-V_f}\left[0.125\left(1.25 + \frac{1}{2}\ln V_f\right) + 0.054V_f - 0.21\sqrt{V_f}\right] \quad (25)$$

Figure 6 represents the variation of the equivalent mean shrinkage in terms of Vf.

Case of partial slip

Determination of the displacements $(U_z)_s$ and $(U_z)_b$: In this case, an expression of σ_{rz} satisfying the matrix-fiber interface conditions is derived. Assuming that the displacement U_r keeps the same form as in the zone z<b, the equations pertaining to the problem permit to get the expression of $(U_z)_s$. All the constants are determined by considering the continuity conditions between the zones of perfect bond and slip.

The expression of $(\sigma_{rz})_s$ can be written as in the following form:

$$(\sigma_{rz})_s = \frac{k_1}{r} + k_3\left(\frac{1}{r} - \frac{r_f}{r^2}\right)z \quad (26)$$

and as U_r vary slightly whether the zone of perfect bond or slip is considered, the expression of $(U_r)_s$ can be written as:

$$(U_r)_s = (U_r)_b = 1.1\varepsilon\left(r - \frac{r_f^2}{r}\right) \quad (27)$$

But

$$(\sigma_{rz})_s = \frac{E}{2(1+\nu)}\left(\frac{\partial(U_r)_s}{\partial z}\right) \quad (28)$$

and comparing with Eq. 27, one gets:

$$(\sigma_{rz})_s = \frac{E}{2(1+\nu)}\frac{\partial(U_r)_s}{\partial r}$$

Hence:

$$\frac{\partial(U_r)_s}{\partial r} = A(\sigma_{rz})_s$$

where:

$$A = \frac{2(1+\nu)}{E}$$

Therefore:

$$(U_z)_s = A\left[k_1 \ln r + k_2\left(\ln r + \frac{r_f}{r}\right)z + k_3(z)\right]$$

where the constants can be determined by using the continuity of the displacements between the two zones (z = b) on one hand and the boundary condition on the other hand: $(\sigma_{rz})_s = \tau_b$ for $r = r_f$.

These constants have the following expressions:

$$k_1 = \tau_b r_f \quad (29)$$

$$k_2 = 0.21\frac{\tau_b}{b} \quad (30)$$

$$k_3(z) = -\frac{\tau_b}{b}(0.25\ln r_f + 0.21)z \quad (31)$$

In a similar manner, the expression $(U_z)_b$ can be given as shown previously by:

$$(U_z)_b = k\left[m\ln\frac{r_f}{r} + n\left(1 - \frac{r_f}{r}\right)\right]z$$

Where:

$k = -\frac{2(1+\nu)}{E}\tau_b$

$m = 0.25$

$n = 0.21$

At this point, one should note that if the continuity of the displacement U_z is satisfied between the zones of perfect bond and partial slip. Then, the continuity of σ_{rz} will be automatically satisfied.

Finally the expression of $(U_z)_b$ and $(U_z)_s$ can be written as:

$$(U_z)_b = -\varepsilon\left[0.25\ln\frac{r_f}{r} + 0.21\left(1 - \frac{r_f}{r}\right)\right]z \quad \text{for } 0 \le z \le b \quad (32)$$

$$(U_z)_s = \frac{2(1+\nu)}{E}\tau_b\left\{r_f \ln r + \left[\begin{matrix}0.21\ln r - 0.25\ln r_f \\ -0.21\left(1 - \frac{r_f}{r}\right)\end{matrix}\right]\frac{z}{b}\right\} \quad \text{for } b \le z \le L \quad (33)$$

where, $b = \frac{1+\nu}{0.02}\tau_b\frac{r_f}{E\varepsilon}$ as given by Eq. 18

Equivalent mean shrinkage: In the case of partial slip along one part of the fiber and perfect bond along the other, the equivalent mean shrinkage can be written:

$$(\varepsilon_{eq})_s = \frac{1}{\varphi}\int\frac{(U_z)_s(l)}{l}d\varphi$$

with $\varphi = \pi(R^2 - r_f^2)$

Replacing $(U_z)_s$ by its expression given in Eq. 33 and integrating, one gets:

$$(\varepsilon_{eq})_s = \frac{4(1+\nu)}{(R^2 - r_f^2)E}\frac{\tau_b}{b}\left\{\begin{matrix}\frac{br_f}{L} + 0.21\left[\frac{R^2}{2}\left(\ln R - \frac{1}{2}\right) - 0.21\left(\frac{R^2 - r_f^2}{2}\right)(1 + \ln r_f)\right] \\ +0.21\, r_f(R - r_f)\end{matrix}\right\}$$

and introducing V_f, it comes:

$$(\varepsilon_{eq})_s = \frac{4(1+\nu)}{(1 - V_f)E}\frac{\tau_b}{b}\left\{\begin{matrix}0.21\left[\sqrt{V_f} - \frac{1}{4}(V_f + 3) - \frac{1}{2}\ln\sqrt{V_f}\right] + \\ \frac{br_f}{2L}\left[(1 - r_f)\ln V_f - \frac{1}{2}(1 - r_f) - \ln\sqrt{V_f}\right]\end{matrix}\right\} \quad (34)$$

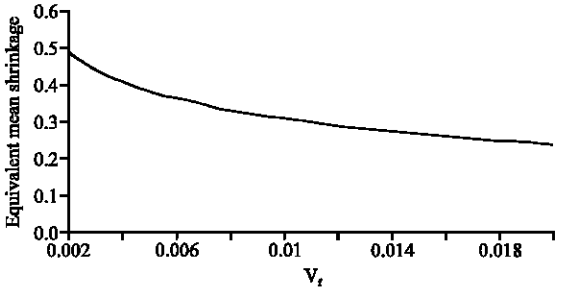

Fig. 6: Effect of Vf on the equivalent mean shrinkage (case of perfect bond)

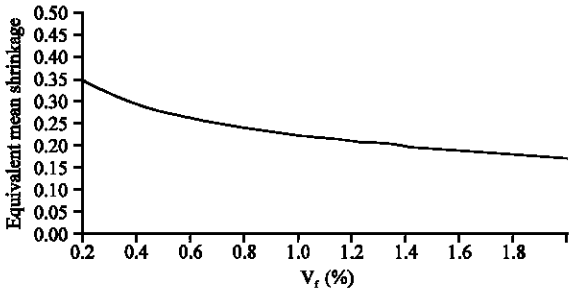

Fig. 7: Equivalent mean shrinkage function of V_f (%) (Sliding along L/2)

If τ_b is replaced by its expression given by Eq. 18, the previous equation becomes:

$$\left(\varepsilon_{eq}\right)_s = \frac{0.08\varepsilon}{(1-V_f)r_f}\left\{\begin{array}{l} 0.21\left[\sqrt{V_f} - \frac{1}{4}(V_f+3) - \frac{1}{2}\ln\sqrt{V_f}\right] + \\ \frac{br_f}{2L}\left[(1-V_f)\ln r_f - \frac{1}{2}(1-V_f) - \ln\sqrt{V_f}\right] \end{array}\right\} \quad (35)$$

By inserting the values of the parameters of the model used in this study, one gets:

$$\left(\varepsilon_{eq}\right)_s = 0.56\varepsilon + 0.15\times10^{-3}\frac{b}{r_f}\varepsilon \quad (36)$$

The effect of the variation of $(\varepsilon_{eq})_s/\varepsilon$ in terms of V_f and the equivalent mean shrinkage for case of perfect bond is shown in Fig .6, while the effect of the variation V_f and the equivalent mean shrinkage considering that slip takes place along one-half of the fiber length (b = L/2) is shown in Fig. 7. It can be seen from Fig. 6 that the equivalent mean shrinkage of a composite material is inversely proportional to the volumetric percentage of the fibers. On the other hand, Fig. 7 shows that in case of slip that takes place along one-half of the fiber length; the value of equivalent mean shrinkage was 0.34 and 0.2 for V_f 0.2% and 2%, respectively, i.e., inversely proportional to the volumetric percentage of the fibers This seems to be logical if the fibers are assumed to be rigid and non-deformable as opposed to the matrix.

CONCLUSIONS

Based on the results of this analytical investigation, the following conclusions are drawn:

- The bond strength is proportional to the bond length
- The bond length is inversely proportional to free shrinkage
- The bond length decreases with age of the composite material
- The equivalent mean length is inversely proportional to the fiber volumetric fraction

REFERENCES

Barluenga, G., 2010. Fiber-matrix interaction at early ages of concrete with short fibers. Cem. Concr. Res., 40: 802-809.

Boghossian, E. and L.D. Wegner, 2008. Use of flax fibres to reduce plastic shrinkage cracking in concrete. Cem. Concr. Comp., 30: 929-937.

Boulekbache, B., M. Hamrat, M. Chemrouk and S. Amziane, 2010. Flowability of fibre-reinforced concrete and its effect on the mechanical properties of the material. Construct. Build. Mater. 10.1016/j.conbuildmat.2010.02.025

Hanayneh, B., 1994. Parametric analysis of fiber-matrix interface in materials with high shrinkage properties. Dirasat Journal, University of Jordan, Vol. 21.

Jay Kim, J.H., C.G Park, S.W. Lee, S.W Lee and J.P Won, 2008. Effects of the geometry of recycled PET fiber reinforcement on shrinkage cracking of cement-based composites. Comp. Part B: Eng., 39: 442-450.

Leung, C.K.Y., M. ASCE, A.Y.F. Lee and R. Lai, 2006. A new testing configuration for shrinkage cracking of shotcrete and fiber reinforced shotcrete. Cem. Concr. Res., 36: 740-748.

Li, F. and Z. Li, 2001. Continuum damage mechanics based modeling of fiber reinforced concrete in tension. Int. J. Solids Struct., 38: 777-793.

Nammur, G. and A. Naaman, 1989. Bond stress model for fiber reinforced concrete based on bond stress-slip relationship. ACI Mater. J., 86: 45-57.

Passuello, A., G. Moriconi and S.P. Shah, 2009. Cracking behavior of concrete with shrinkage reducing admixtures and PVA fibers. Cem. Concr. Comp., 31: 699-704.

Sivakumar, A. and M. Santhanam, 2007. A quantitative study on the plastic shrinkage cracking in high strength hybrid fibre reinforced concrete. Cem. Concr. Comp., 29: 575-581.

Toledo Filho, R.D., K. Ghavami, M.A. Sanjuan and G.L. England, 2005. Free, restrained and drying shrinkage of cement mortar composites reinforced with vegetable fibers. Cem. Concr. Comp., 27: 537-546.